

## The climatological minimum in tropical outgoing infrared radiation: Contributions of humidity and clouds

By STEPHEN G. WARREN

*Dept. of Atmospheric Sciences AK-40, University of Washington, Seattle, WA 98195 U.S.A.*

and

STARLEY L. THOMPSON

*National Center for Atmospheric Research,<sup>1</sup> Boulder, Colorado 80307 U.S.A.*

(Received 18 November 1981; revised 28 July 1982)  
(Communicated by Dr F. Bretherton)

### SUMMARY

Satellite observations of outgoing terrestrial infrared (IR) radiation as a function of latitude exhibit a minimum near the equator  $20\text{--}40\text{ W m}^{-2}$  smaller than peaks in the subtropics. We attempt to dissect the causes of the dip through calculations with a spectrally-detailed multi-level radiative transfer model. Roughly one third of the dip can be attributed to the latitudinal variation of atmospheric water vapour; the remainder apparently is due to latitudinal variations in cloud amount and (especially) cloud-top height. However, inclusion of clouds as given by published climatologies enhances the clear-sky dip only slightly. Thus, about one half of the dip is essentially unexplained. We suspect the explanation is that near-equatorial cirrus and cumulonimbus heights are too low in the cloud climatology, emphasizing the need for a better cloud climatology.

Since tropospheric humidity variations have a strong effect on clear-sky outgoing IR, empirical studies which correlate cloud with IR variations may overestimate the effect of clouds on outgoing IR if cloud amount is correlated with relative humidity.

The effect of humidity variations on outgoing IR suggests that a measure of tropospheric humidity be incorporated explicitly in the parametrization of outgoing IR for simple climate models.

### 1. INTRODUCTION

Observations from satellites of thermal infrared (IR) radiation (wavelength  $\lambda \gtrsim 4\ \mu\text{m}$ ) escaping the earth-atmosphere system, when plotted as a function of latitude, show not a single broad peak in the warm tropical region but rather two peaks with a local minimum between them. This is prominent for zonal averages, where the peak-to-valley difference is  $20\text{--}40\text{ W m}^{-2}$  depending on time of year. The minimum is located near the equator and moves north and south with the seasons to about  $\pm 7^\circ$  latitude. It is seen both in the narrow-band  $10.5\text{--}12.5\ \mu\text{m}$  measurements (Fig. 3 of Gruber and Winston 1978) and in the energy-budget measurements of the entire thermal infrared spectrum (Campbell and Vonder Haar 1980; plotted below in Fig. 6). Campbell and Vonder Haar show, for two years of Nimbus-6 data, a dip ranging from  $21\text{ W m}^{-2}$  (December) to  $40\text{ W m}^{-2}$  (August). The Nimbus-6 spatial resolution was only  $10\text{--}15^\circ$  of latitude; the observed reduction is greater if higher-resolution data are used: Nimbus-3 observations at  $2.5^\circ$  resolution for May 1969 show a dip of  $39\text{ W m}^{-2}$  (Campbell, personal communication). [Since the Nimbus-6 satellite samples all parts of the earth at the same local time, it may not obtain the absolute value of the diurnal average outgoing IR accurately, but the magnitude of the *dip* should be relatively unaffected by this temporal sampling bias.]

Since zonally averaged temperatures do not show such a double peak in any season, neither for surface temperatures (Table 1a of Warren and Schneider 1979) nor for atmospheric temperatures (Oort and Rasmusson 1971 and Taljaard *et al.* 1969), the dip must be due to the increased infrared opacity of the atmosphere near the zonally averaged location of the ITCZ, a region which is both cloudier and more humid than the zones  $20^\circ$  to the north or south.

The dip is normally attributed to clouds (e.g. Gruber and Winston 1978, Stephens *et al.* 1981). We attempt here to dissect its cause through calculations with an atmospheric

<sup>1</sup> The National Center for Atmospheric Research is sponsored by the National Science Foundation.

radiation model, and we show that about one third of the dip can be attributed solely to changes of humidity with latitude; the remainder we attribute, by default, to changes of cloud amount and height with latitude.

## 2. MODEL DESCRIPTION

Outgoing IR at the top of the atmosphere is estimated using the atmospheric radiation model of Wiscombe (1975). This model employs the exponential-sum-fitting-of-transmission-functions method (reviewed by Wiscombe and Evans 1977) to handle line absorption. This method allows spectral intervals containing many absorption lines to be treated reasonably correctly even when there is scattering or surface reflection (the latter is important in the long-wave when surface emissivity  $\varepsilon < 1$ ). However, the model was employed in the present context only for clear skies or black-body clouds, so the power of its adding-doubling scattering formalism was never used; only the no-scattering limit for the Planck function source doubling (Wiscombe 1976) was needed. In this circumscribed usage the model is like other sophisticated long-wave models (e.g. Ellingson and Gille 1978) save in one respect: because it treats properly the diffusion or optically-thick limit (see Wiscombe 1976), it is not necessary to take very small vertical steps. In fact, for all our calculations we use only the 31 levels in the well-known McClatchey *et al.* (1972) model atmospheres: 1 km steps up to 25 km and then 5 km steps up to 50 km. We employ 136 spectral intervals spanning  $3 \leq \lambda \leq 500 \mu\text{m}$ , since the model was already set up for such a spectral resolution. A coarser resolution would have been satisfactory but would have entailed making a new exponential-fit table. The transmission functions are principally those of LOWTRAN 5 (Kneizys *et al.* 1980); this, however, includes the water vapour continuum of Roberts *et al.* (1976) only for  $7 < \lambda < 15 \mu\text{m}$ . In Wiscombe's model the continuum absorption for the entire spectral range measured by Burch (Burch and Gryvnak 1979), i.e.  $7 < \lambda < 30 \mu\text{m}$ , has been included using the empirical fit given by the solid line in Fig. 2 of Roberts *et al.* This continuum absorption is proportional to the square of the water vapour concentration. It is due to absorption by  $(\text{H}_2\text{O})_2$  or to self-broadened wings of strong lines in the  $\text{H}_2\text{O}$  rotation band at  $\lambda > 30 \mu\text{m}$ , and is included in addition to other water vapour absorption lines whose centres are in the 7–30  $\mu\text{m}$  region. The water vapour continuum absorption assumed is that of Roberts *et al.*, including the temperature dependence which they state is too strong for  $\lambda > 20 \mu\text{m}$ , but with the modifications of Selby *et al.* (1976, Eq. 6). The absorption decreases with increasing temperature, due either to the expected dissociation of dimers with increasing temperature or to weaker interactions during collisions of  $\text{H}_2\text{O}$  molecules with each other at higher temperature. Roberts *et al.* suggested omitting the foreign-broadened component of the continuum which had been previously used, but Selby *et al.* recommended including it at a reduced level, based on measurements shown in their Fig. C1. This temperature-independent foreign broadening is included, as is the  $\text{H}_2\text{O}$  continuum in the 4  $\mu\text{m}$  region (where there is, however, little contribution to the outgoing infrared) as given by Eqs. 5 and 9 of Selby *et al.* This water vapour continuum absorption is essentially similar to what will be included in the new LOWTRAN 6, which will be based on measurements of the continuum (and calculations for the far-wing line shapes) over most of the spectrum from the visible to the microwave, both pressure-broadened and self-broadened (Kneizys, personal communication to Wiscombe, 1981). [In Fig. 3 below we investigate the relative contributions of water vapour line absorption and continuum absorption to the tropical dip in outgoing long-wave radiation.]

## 3. ZONAL AVERAGE ATMOSPHERIC PROFILES

The calculations all use zonally averaged vertical profiles of temperature and ozone (at 5° latitude intervals) for January and July. Standard humidity profiles are also defined

from which specified deviations are taken in some of the model experiments. The surface emissivity is assumed to be 0.95, independent of wavelength – intermediate between the extremes of 0.90 for sand desert and 0.99 for snow, measured by Griggs (1968) in the 8–14  $\mu\text{m}$  region. The emissivity of a water surface in this spectral region is about 0.95 according to calculations of Miranova (1973, her Table 4.44). Outside the 8–14  $\mu\text{m}$  window the possible variation of surface emissivity has little effect on outgoing IR from the surface unless there is a temperature discontinuity at the surface, because emissivity and reflectivity add to unity.

Construction of the standard profiles of temperature, ozone and water vapour is described by Thompson and Warren (1982) and also in section 4 below.

For specifying perturbed relative humidity (RH) profiles used in some of the model experiments, we find it useful to define a measure of average tropospheric humidity to characterize the entire profile. Thompson and Warren find that a key humidity parameter sufficient to predict clear-sky outgoing IR without knowledge of the lapse rate of temperature is  $\widehat{\text{RH}}$ , which is the height-mean (not pressure-mean) relative humidity for the atmospheric layer 0–12 km. Figure 1 shows the zonally averaged value of this parameter as a function of latitude for January and July. It has minima in both the north and south subtropics and a maximum of about 57% near the equator.

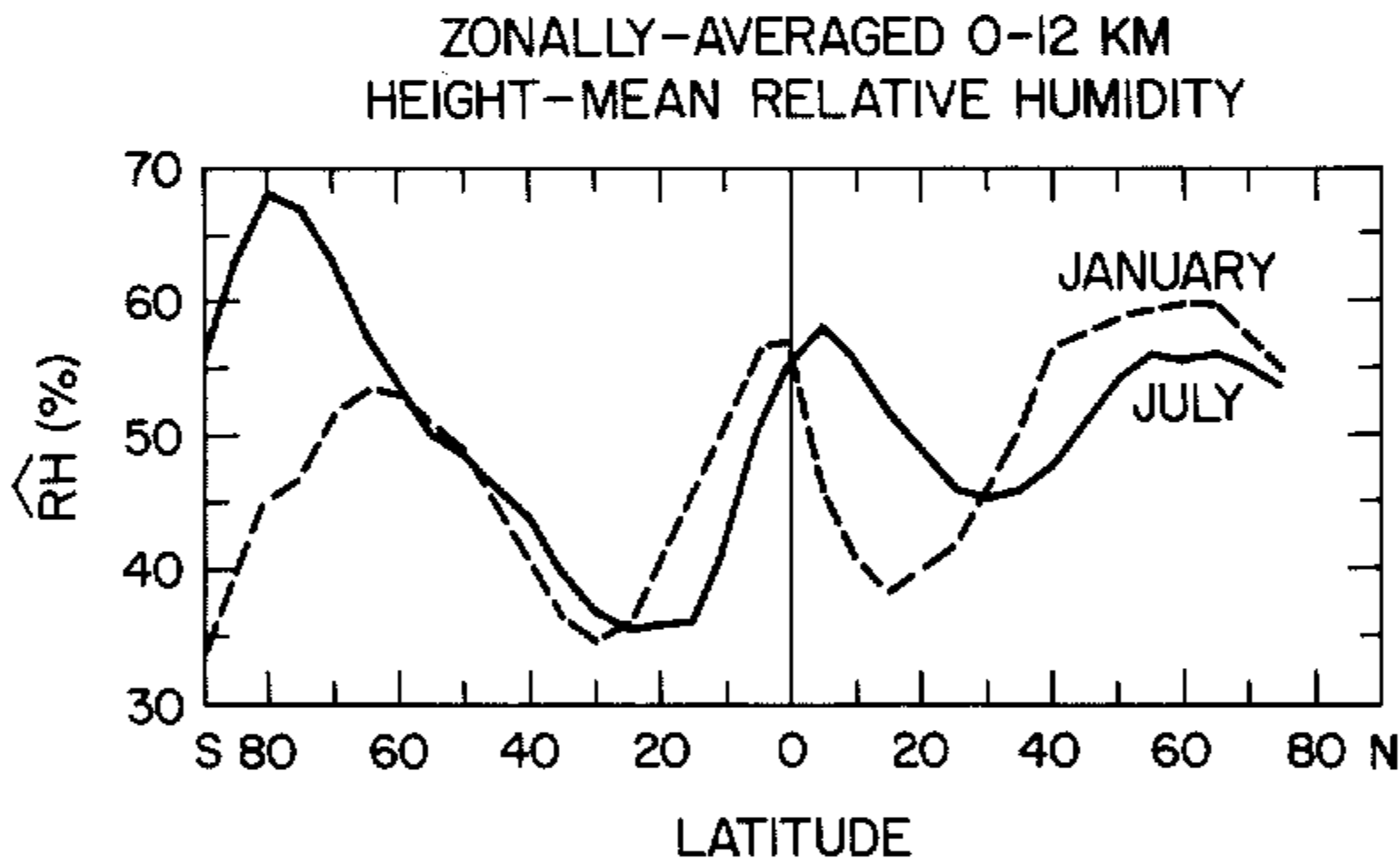


Figure 1. Zonal average mean tropospheric relative humidity,  $\widehat{\text{RH}}$ , defined as the height-mean for 0–12 km. Data sources are given in section 4.

The values of RH and  $\widehat{\text{RH}}$  used in this study are likely to be significantly different from correct climatological values. For the southern hemisphere, monthly mean temperatures and dew-point temperatures from Taljaard *et al.* (1969) were used to compute RH. This procedure typically underestimates the monthly mean by about 0.05. For the northern hemisphere monthly mean specific humidities and temperatures by Oort and Rasmusson (1971) were used. In contrast to the southern hemisphere this procedure tends to overestimate monthly mean RH. Indeed, a bias towards higher RH in the northern hemisphere is evident for mid-latitudes and the subtropics in Fig. 1. There is clearly a need for a better climatology of RH as a function of season, latitude and height. Where calculations in this paper are compared with satellite observations, part of any discrepancy is likely to be due to incorrect specification of RH.

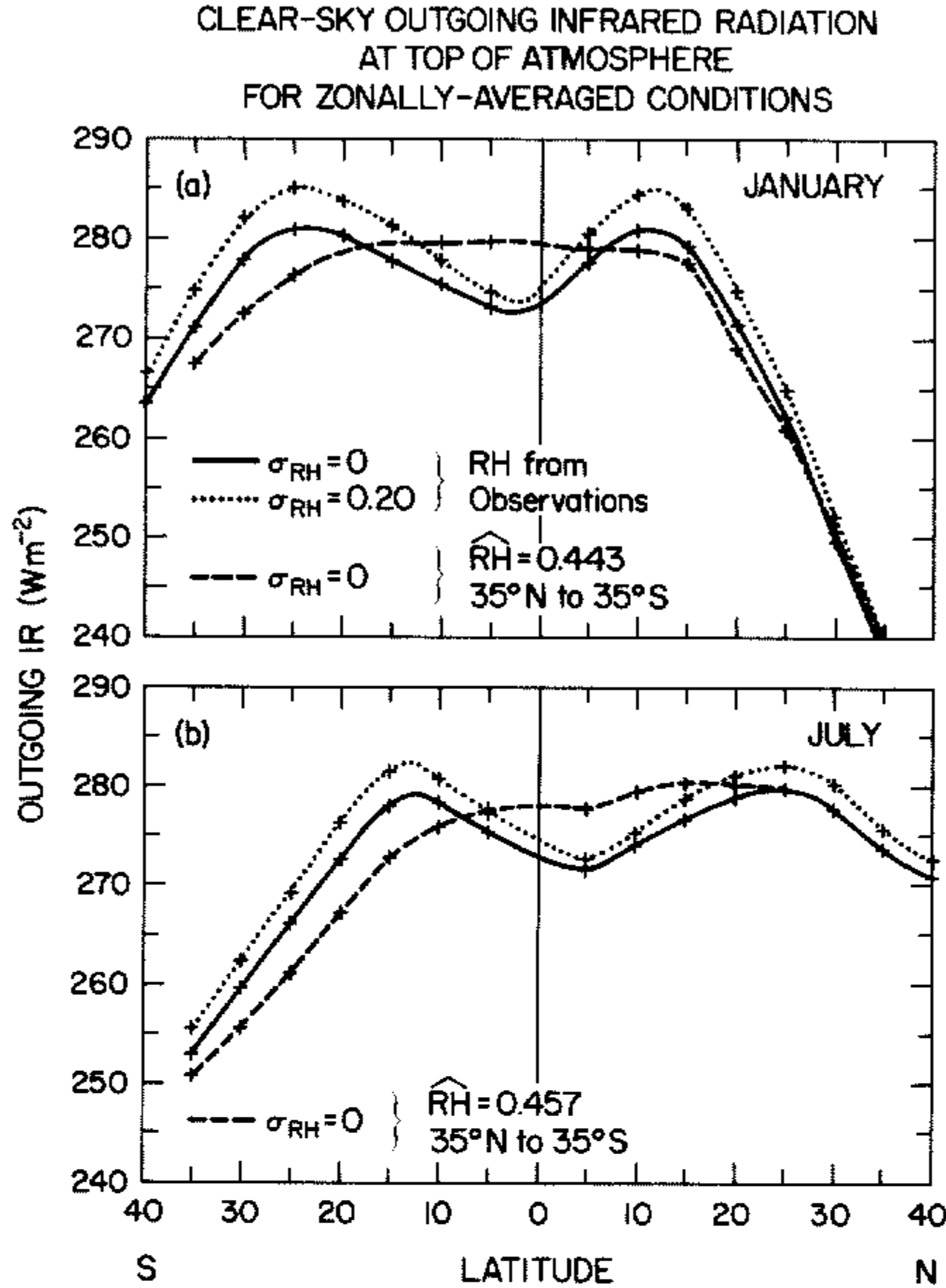


Figure 2. Clear-sky outgoing infrared radiation calculated with a detailed radiative transfer model for zonally-averaged temperature, water vapour, and ozone profiles, for (a) January and (b) July.

*Solid lines:* Standard profiles, no day-to-day variation of relative humidity. Calculations were made at points marked '+' and a smooth curve drawn through the points. *Dotted lines:* Day-to-day variation of RH was assumed to be given by  $\sigma(RH) = 0.2$ . Outgoing IR was calculated from profiles at standard  $\widehat{RH}_0$ , and at  $\widehat{RH}_0 \pm (\sigma, 2\sigma)$ . A weighted average outgoing IR is reported. *Dashed lines:* The mean value of RH was calculated for the entire band of zones 35°N to 35°S. The vertical RH profiles at each latitude were then shifted as described in the text until RH reached that mean value. Outgoing IR was calculated from these perturbed profiles.

#### 4. INFLUENCE OF RELATIVE HUMIDITY ON THE IR DIP

Model calculations of *clear-sky* outgoing IR in the tropics are shown in Fig. 2. Standard profiles of temperature, ozone, and water vapour are constructed as follows. Surface air temperatures are given in Table 1a of Warren and Schneider (1979). Atmospheric temperatures for 1–22 km are taken from Taljaard *et al.* (1969) for 0 to 85°S and from Oort and Rasmusson (1971) for 5 to 75°N. Values for our height levels are interpolated from the values given at pressure levels by integrating the hydrostatic equation with knowledge of the zonal mean surface elevation. Temperatures at 50 mb for the northern hemisphere are assumed to apply with seasonal reversal to the southern hemisphere (where the data of Taljaard *et al.* do not extend above 100 mb) except for 80 to 90°S, where temperatures are obtained by interpolation between temperatures at 75°S and the

south polar 50 mb temperatures in Fig. 6 of Crutcher (1969). Temperatures and relative humidities above 22 km are taken from the model atmospheres of McClatchey *et al.* (1972), interpolated in latitude,  $\phi$ , for  $15^\circ < |\phi| < 70^\circ$  with the assumption that 'sub-arctic' profiles apply to  $|\phi| \geq 70^\circ$ , 'mid-latitude' to  $|\phi| = 45^\circ$ , and 'tropical' to  $|\phi| \leq 15^\circ$ . Ozone profiles are taken from a similar interpolation of the McClatchey model atmospheres.

Zonal average relative humidities below 22 km are either taken or derived from Oort and Rasmusson (1971) for 0–7 km,  $10^\circ\text{S}$  to  $75^\circ\text{N}$ ; from London (1957) for 7–22 km, 0 to  $75^\circ\text{N}$ ; and from Sasamori *et al.* (1972) for 0–22 km, 10 to  $90^\circ\text{S}$  and 7–22 km, 0 to  $10^\circ\text{S}$ . The Oort–Rasmusson data are retained to  $10^\circ\text{S}$  in order to use an internally consistent set of RH across the region of the tropical IR minimum. At  $\phi = 10^\circ\text{S}$ , 0–7 km we average the values reported by Sasamori *et al.* and by Oort and Rasmusson to ensure continuity. [We do take exception to some of the Oort–Rasmusson values at the surface in the arctic winter where combinations of temperature, pressure and water vapour mixing ratio imply RH over ice greater than 100%. In such cases we set the RH to 100%.]

Consider first the solid lines (discussion of  $\sigma(\text{RH})$  is deferred to section 5): a tropical dip of  $\sim 8 \text{ W m}^{-2}$  is predicted for both January (at  $2^\circ\text{S}$ ) and July (at  $5^\circ\text{N}$ ) using observed zonally averaged profiles.

We now show that this dip is due to the latitudinal variation of relative humidity. The average value of  $\hat{\text{RH}}$  from  $35^\circ\text{N}$  to  $35^\circ\text{S}$  is 44% in January and 46% in July, but Fig. 1 shows that there is considerable variation with latitude. Now, instead of using the true atmospheric water vapour profiles, we shift each of those profiles to higher or lower humidity as necessary until all have the same  $\hat{\text{RH}}$  (44% for January; 46% for July). This we do in an individual profile by adjusting RH by the same amount at all levels up to 12 km. (However, RH at any level is limited to  $\leq 100\%$  and the water vapour mixing ratio is required to be at least the assumed stratospheric value of  $2.5 \times 10^{-6}$ .) Temperatures in these zonally averaged profiles are not changed.

The dashed lines in Fig. 2 show the outgoing IR for these new profiles. The dip has disappeared, making it clear that it is the mean tropospheric relative humidity,  $\hat{\text{RH}}$ , which is responsible for the  $8 \text{ W m}^{-2}$  dip.

As mentioned above, the absorption of long-wave radiation by water vapour is partially continuum, 'e-type', absorption. Since this absorption is proportional to the square of the water vapour concentration, it is expected to be most important in the tropics. Figure 3 shows the contribution of continuum absorption to reducing the outgoing IR in the tropics. The solid lines in Figs. 2 and 3 are identical; the dashed line shows the result of omitting the water vapour continuum from the calculations. The continuum is indeed most important in the tropics where it accounts for as much as  $10 \text{ W m}^{-2}$  of the water vapour 'greenhouse effect', but its contribution is not negligible even at  $40^\circ\text{N}$  in winter, where it still accounts for  $1.2 \text{ W m}^{-2}$ . The dip is reduced from  $8.1$  to  $4.6 \text{ W m}^{-2}$  (on average) if we omit continuum absorption, so that continuum absorption can be considered responsible for about 40% of the clear-sky dip.

##### 5. INFLUENCE OF TIME-VARIATIONS IN RELATIVE HUMIDITY AND SURFACE TEMPERATURE

Because the wavelength-integrated infrared emission is proportional to the fourth power of temperature, and temperature generally decreases monotonically with height in the troposphere, day-to-day variations in  $\hat{\text{RH}}$  which raise or lower the effective level of emission to space cause the time-averaged outgoing IR to be *greater* than it would be for a non-varying  $\hat{\text{RH}}$  fixed at its time-averaged value. This effect is shown below to be larger for low  $\hat{\text{RH}}$ , so it will tend to enhance the dip.

The effect on zonal average outgoing IR is of course due both to temporal variability

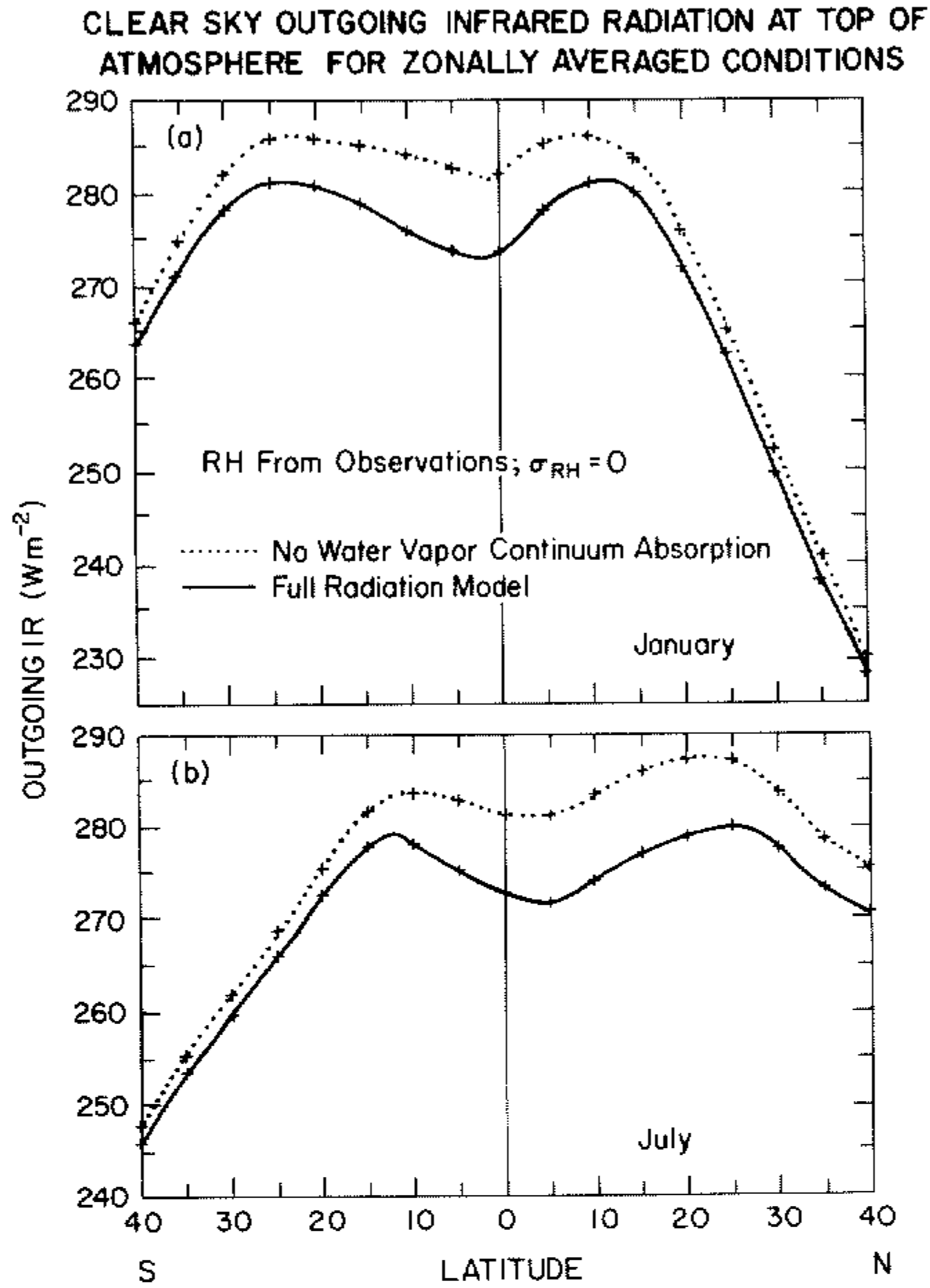


Figure 3. Effect of water vapour continuum (e-type) absorption on outgoing IR radiation, using standard climatological zonally averaged atmospheric profiles (ignoring day-to-day and longitudinal variations of RH). *Solid lines:* Calculations using the complete radiation model. These lines are identical to the solid line in Fig. 2. *Dotted lines:* Calculations omitting water vapour continuum absorption but including  $\text{H}_2\text{O}$  line absorption.

at a particular location and to spatial variation around the zone. We estimate only the temporal variability here, so the true effect will be larger than calculated. The effect arises from changes in  $\hat{R}\hat{H}$  which are due to changes in water vapour mixing ratio, not those due solely to changes in temperature. We therefore do not consider the large day-night changes in  $\hat{R}\hat{H}$  which are due to concerted changes of lower tropospheric temperature and RH but leave absolute humidity largely unaltered; we study only day-to-day variability. An estimate of the day-to-day variability of  $\hat{R}\hat{H}$  is obtained from radiosonde data and general circulation model simulations, as described in the appendix. The estimated standard deviation is given by  $\sigma(\hat{R}\hat{H}) \approx 0.20$ , which we now use to simulate the effect of RH variability on outgoing IR.

Outgoing IR was calculated for each  $5^\circ$  latitude zone for that zone's standard profile of mean tropospheric relative humidity,  $\hat{R}\hat{H}_0$ , and for four perturbed profiles with  $\hat{R}\hat{H} = \hat{R}\hat{H}_0 \pm (0.2 \text{ or } 0.4)$  (i.e.  $\hat{R}\hat{H}_0$  perturbed by one or two standard deviations). The RH

profiles are perturbed by equal amounts at all levels below 12 km, except for the restrictions in maximum and minimum values previously noted. [These vertically uniform perturbations should be adequate because Fig. 6 of Thompson and Warren (1982) shows that outgoing IR is affected primarily by RH, and only slightly by the detailed profile of RH.] The average outgoing IR is obtained by taking a weighted average of the five IR values, weighted according to a normal distribution. Figure 4 shows the difference between this average and the outgoing IR for the standard climatological average RH

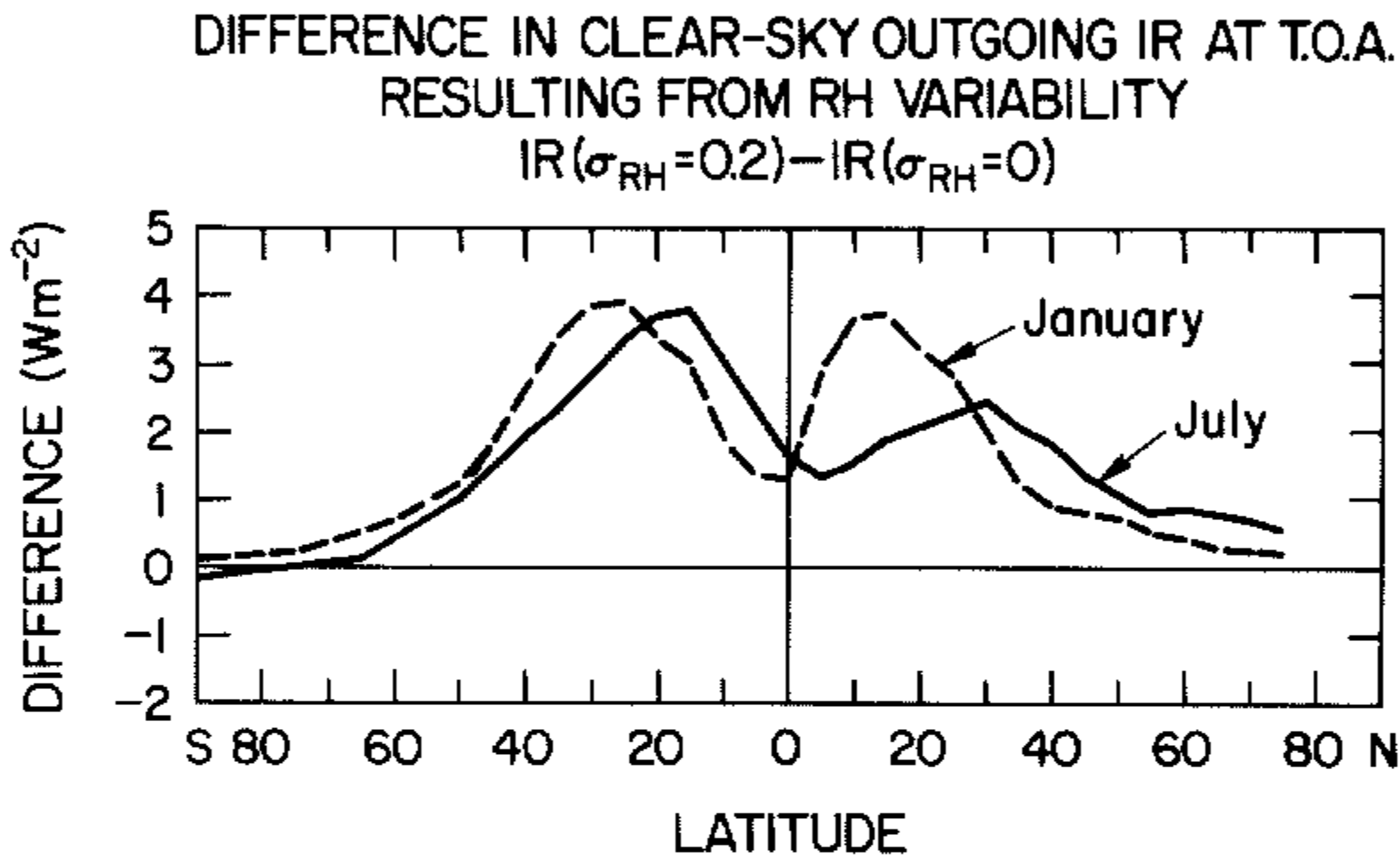


Figure 4. Difference in calculated clear-sky outgoing IR radiation at the top of the atmosphere resulting from day-to-day variability of relative humidity. Standard deviation of RH was taken to be either 0.2 or zero. Calculation procedure is given in the text.

profile. The difference is positive except for the antarctic winter, where the effective radiating level happens to be close to the top of the inversion layer in the standard case, so that both positive and negative RH perturbations give rise to lower effective radiating temperatures. The difference is larger in the subtropics than at the equator by an average of  $2 \text{ W m}^{-2}$ . This increases the magnitude of the clear-sky dip to an average of  $10 \text{ W m}^{-2}$ , shown by the dotted lines in Fig. 2.

This exercise illustrates the effect on outgoing IR of variability in RH. The effect would be larger if variations with longitude as well as with time were considered. Such a study awaits a better global climatology of relative humidity and its variations.

The diurnal variation in surface temperature also biases outgoing IR. However, the effect is seen to be small by the following argument. Assuming that atmospheric temperatures and absolute humidities undergo no diurnal variation and that surface temperatures vary, say, between 310 and 290 K from day to night, there is a 0.7% bias in IR emitted from the surface relative to a constant temperature of 300 K. The effect is smaller at the top of the atmosphere because surface emission is then multiplied by atmospheric transmissivity. Thompson and Warren (1982) find that the maximum contribution of the surface to the outgoing IR for any of the standard McClatchey *et al.* profiles is  $70 \text{ W m}^{-2}$  (mid-latitude winter). Thus the error we may incur by ignoring day-night surface temperature changes is only about  $0.5 \text{ W m}^{-2}$ .

## 6. INFLUENCE OF CLOUDS ON THE IR DIP

Because of the lack of an accurate global climatology of cloud amounts and cloud-top heights, we make a number of simplifying assumptions in specifying cloud conditions for model calculations. For a black cloud or a grey cloud, Ramanathan (1977, Fig. 4) has shown that the modulation of outgoing IR by clouds is essentially a linear function of the difference between surface and cloud-top temperatures,  $(T_s - T_c)$ . This linear relation allows one to combine multi-level clouds into a single effective cloud layer. From published reports we estimate a zonal average total cloud amount and an average  $(T_s - T_c)$  for a single effective 'black' cloud layer. For radiative transfer calculations we insert a cloud layer with emissivity of 100% at the level whose temperature is  $T_c$ .

The zonally averaged total cloud cover for January and July is taken from London (1957) for the N.H. and from van Loon (1972) for the S.H. In order to avoid a discontinuity at the equator we use Murakami's (1975) zonal cloud amounts for 25°N to 25°S. Murakami obtained these by averaging zonally the (unpublished) satellite nephanalyses of J. C. Sadler and co-workers (University of Hawaii). They give an average cloud cover for 25°N–25°S which is within 0.02 of those given by London and by van Loon. The values assumed are given in Table 1.

TABLE 1. ZONAL AVERAGE TOTAL CLOUD COVER ASSUMED IN CALCULATIONS OF OUTGOING IR

Zonal average total cloud cover taken from London (1957) for 30 to 75°N, from Murakami (1975) for 25°N to 25°S, and from van Loon (1972) for 30 to 75°S.

Latitude zone centred at	Total cloud cover (%)	
	January	July
75°N	47	69
70	52	68
65	58	66
60	60	65
55	63	63
50	61	59
45	59	55
40	54	48
35	50	41
30	44	41
25	44	43
20	41	45
15	39	49
10	42	58
5	51	56
0	51	50
5	53	48
10	53	47
15	52	47
20	50	48
25	49	49
30	48	48
35	52	55
40	57	59
45	65	65
50	75	72
55	82	78
60	85	80
65	84	76
70	74	61
75°S	61	46

The zonally averaged ( $T_s - T_c$ ) is obtained as follows. London (1957, Table A-3) reported relative amounts and base heights of clouds grouped into six cloud-type categories for winter and summer in N.H. zones. (More detail is given in Fig. 15 of Telegadas and London (1954).) We assume that cirrus is thin. Cumulonimbus tops we assume to have the same height as cirrus tops. Stratus, cumulus, altostratus and nimbostratus are all assumed for convenience to be 1 km thick. All clouds are assumed black except for cirrus, which is assigned an emissivity of 0.5 independent of wavelength. [In practice, to form the single effective black cloud, we halve cirrus amount rather than cirrus emissivity.] Cirrus emissivity is discussed critically below.

Temperatures corresponding to these cloud-top heights are obtained from London's tables of tropospheric temperatures. The three cloud layers (low, middle, high) are assumed to overlap randomly, except that middle cloud nimbostratus and low cloud stratus are assumed not to overlap since their bases occur at the same height. Together with surface temperatures, this procedure yields a set of winter and summer zonal values of ( $T_s - T_c$ ) for the N.H. which are plotted in Fig. 5.

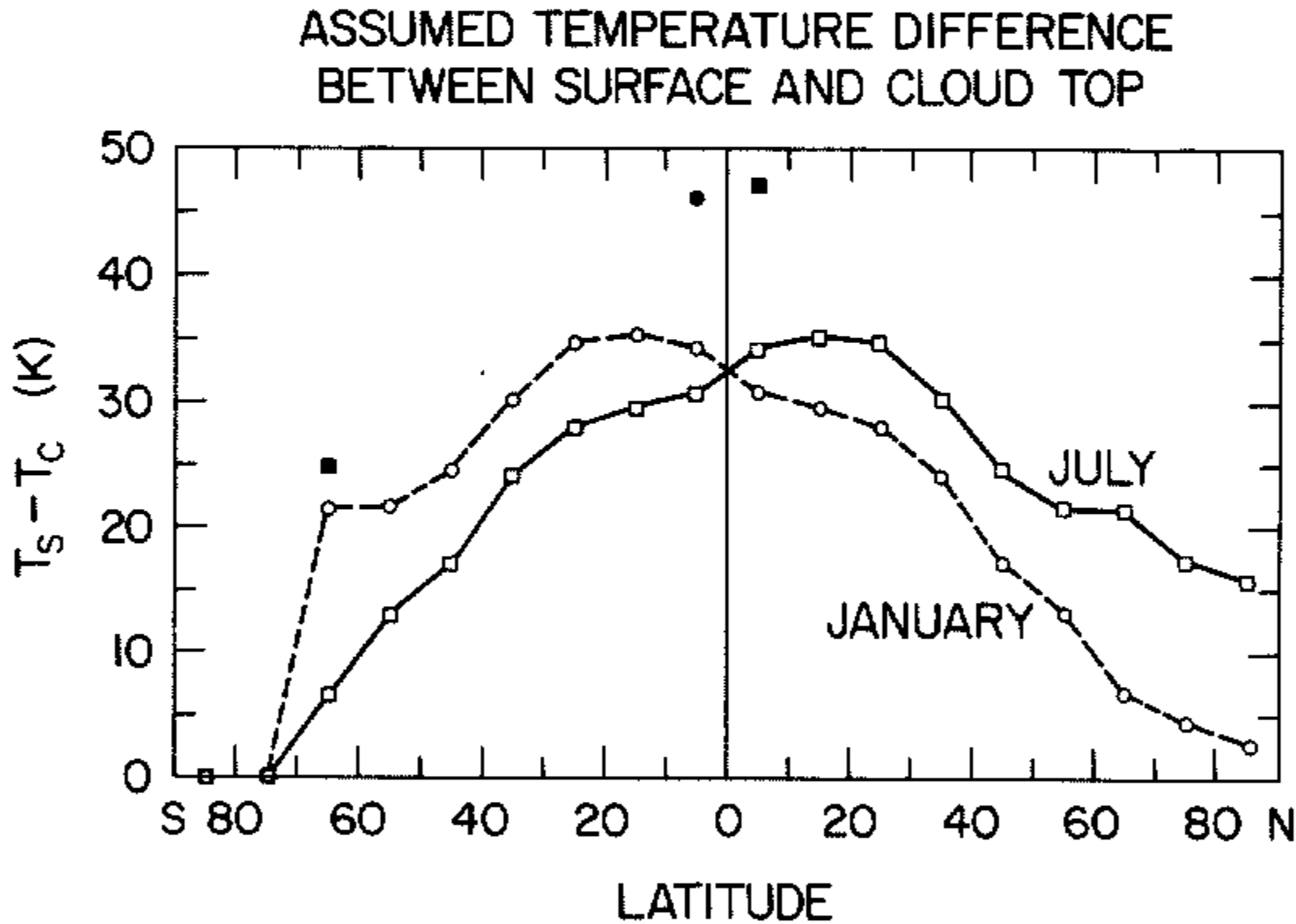


Figure 5. Assumed zonal average temperature difference between surface and cloud top. The height of a single effective 'black' cloud was obtained as described in the text, based on cloud heights given by London (1957).

These are plotted as open symbols connected by lines: square = July, circle = January.

*Solid symbols:* Values of ( $T_s - T_c$ ) necessary to reconcile radiative model calculation with satellite observation shown in Fig. 6. These are shown only for the three cases giving the worst discrepancies in Fig. 6.

Values of ( $T_s - T_c$ ) for the S.H. are assumed to be the same as those for N.H., with seasonal reversal, except for Antarctica where ( $T_s - T_c$ ) is taken to be zero in both seasons. We thus assume that clouds have no effect on outgoing IR over Antarctica. This is because there the clouds are optically thin (due to the low absolute humidity) and because the temperature lapse rate is small.

The IR radiative transfer calculations are performed for the zonal average profiles (ignoring temporal variability of RH) both with and without cloud, and the results averaged according to the climatological cloud cover. Outgoing IR is smaller at all latitudes relative to clear-sky values, as shown in Fig. 6.

It is surprising that the dip is increased only slightly by the addition of clouds, from

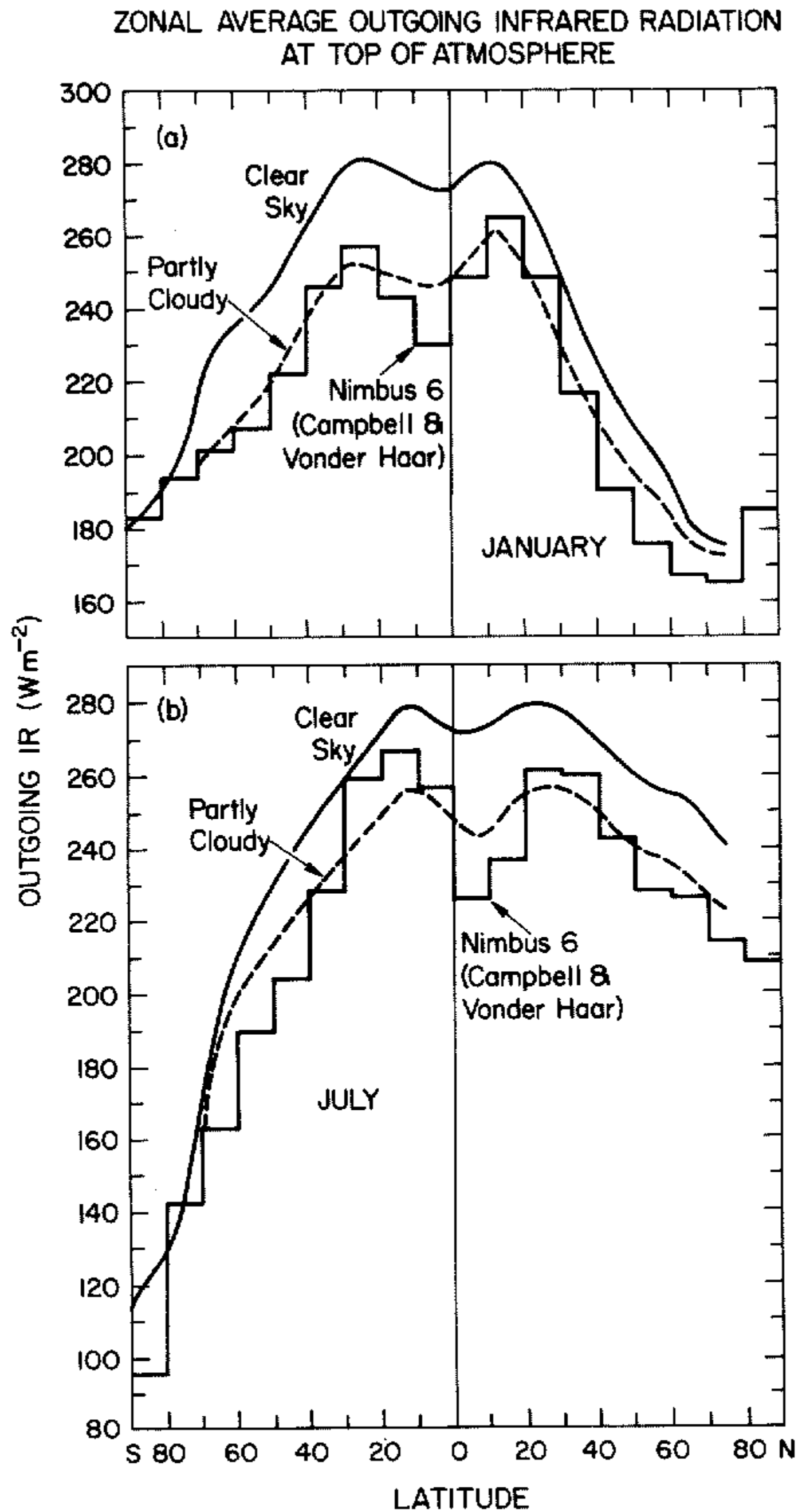


Figure 6. Zonal average outgoing infrared radiation at the top of the atmosphere: comparison of model calculation with satellite observation.

*Solid lines:* Standard profiles for clear sky. These are the same as the solid lines in Fig. 2. Calculations were made at  $5^\circ$  latitude intervals and a smooth line drawn through the points. *Dashed lines:* Weighted average of outgoing IR calculated for clear-sky conditions and for the same profiles but with a black cloud inserted at a level according to Fig. 5. For the average, the two IR values were weighted according to the zonal average cloud amount given in Table 1. *Histogram:* Zonal average total outgoing infrared radiation measured by Nimbus 6 for January 1976 and 1977 and July 1975 and 1976. Each histogram is the average of two months.

8.2 to 12.3  $\text{W m}^{-2}$  for the January–July average. Observations from Nimbus 6 reported by Campbell and Vonder Haar (1980) are also plotted in Fig. 6 and show that the observed dip is much larger than the dip we calculate. Stephens *et al.* (1981) have performed infrared radiative transfer calculations for annual average, zonally averaged atmospheric conditions. In contrast to our results for individual months, they are able to match the mean annual IR fluxes rather well. They did not attempt to separate the effects of cloud and humidity, but their data sources for temperature, humidity and cloud differed little from ours. Their Fig. 16 shows a calculated tropical dip of 14  $\text{W m}^{-2}$ , i.e. about the same as we calculate, but an observed dip of only 17  $\text{W m}^{-2}$ . This is much smaller than the dip shown in our Fig. 6 for individual months because the dip moves north and south with the seasons. Stephens *et al.*'s apparent good agreement between model and observations for mean annual conditions obscures the large discrepancies that occur in individual months.

The discrepancy we find between observed and calculated outgoing IR is likely to be in our specifications of cloud amount, cloud height and cloud emissivity. Fractional cloud amounts may actually be as much as 0.08 higher at 5°N and 5°S than reported by London (1957), van Loon (1972) and Murakami (1975), at least over the oceans, according to analyses of ship observations for 1946–1978 reported by Warren *et al.* (1981, and personal communication). Use of the larger cloud amounts would reduce the outgoing IR shown in the 'partly cloudy' curves in Fig. 6 for January 5°S and July 5°N by only 3–4  $\text{W m}^{-2}$ , with  $(T_s - T_c)$  as given by Fig. 5. Thus most of the discrepancy between observation and calculation probably comes not from error in cloud amount but rather from error in cloud height and emissivity, which influence the effective  $(T_s - T_c)$ .

There is also an error in the assumption about how cloud layers overlap. The random-overlap assumption is valid only for instantaneous cloud conditions at a point. The overlap of time-averaged cloud layer amounts is likely to be intermediate between random overlap and no overlap. The no-overlap assumption would give values of  $(T_s - T_c)$  2–4 K smaller than those plotted in Fig. 5. Thus, the error of the random-overlap assumption cannot explain the discrepancy between computed and observed outgoing IR, because the assumption actually increases the magnitude of the dip, compared with no-overlap.

The largest errors are at 5°S in January and at 5°N and 65°S in July. We have computed values of  $(T_s - T_c)$  necessary, in these three cases, to match observations. The required values are plotted as solid dots in Fig. 5. They suggest that cirrus and cumulonimbus tops at the ITCZ are much higher (and therefore colder) than London reported; or that cirrus at the ITCZ is thicker than we have assumed, so that its emissivity is greater than 0.5; or that tropical cirrus amounts are larger than the 23% given by London. All these are possible.

Analysis of outgoing IR in the tropics measured by NOAA scanning radiometers (with the high spatial resolution not available in Nimbus-6 data) shows that the largest difference in equivalent blackbody temperature from one 2.5° latitude–longitude box to another is typically 80 K (Riehl and Miller 1978, Short and Wallace 1980). Furthermore, if cirrus in the ITCZ originates mainly in cumulonimbus tops, it may well be thicker than cirrus typical of higher latitudes, and thus have higher emissivity. Such low temperatures for tropical cumulonimbus anvils were also routinely found in U-2 flights over Panama and northern South America and nearby oceans by Danielsen (1982). Furthermore, he reported a diurnal maximum area of 4–6% covered by anvils of brightness temperature  $< -76^\circ\text{C}$ , implying emissivity  $\epsilon > 0.96$ ; the emissivity decreases with increasing distance from the anvil centre. If this is typical of the tropics, our assumed average emissivity of 0.5 for cirrus is too low.

Emissivity of cirrus clouds is a subject of active research. Cox (1971, 1976) found, from balloon-borne radiometersondes, that the emissivity of tropical cirrus was larger ( $\sim 0.7$ ) than that of mid-latitude cirrus ( $\sim 0.6$  for clouds at 500 mb, decreasing to 0.1 for

clouds at 300 mb). Griffith *et al.* (1980) measured infrared irradiances from aircraft above, below, and within tropical cirrus cloud in the GATE. They found that three different clouds (ranging from a thin cloud to an anvil) all exhibited the same variation of  $\varepsilon$  with depth,  $\varepsilon$  reaching 0.9 at 1 km depth. They also found that the radiative models of Hunt (1973) and Liou (1974) consistently underestimated the emissivity for a given cloud ice-water content. This led them to conclude that 'tropical cirrus cloud emissivities may be significantly larger than heretofore believed.' The subject of cirrus emissivity is unfortunately confused by the use of a variety of operational definitions, discussed by Platt and Stephens (1980). In particular, Stephens (1980) commented that these apparent discrepancies between model and observation were partly due to the inclusion of infrared reflection in the 'apparent emissivity' of Griffith *et al.*

Our assumed cirrus amounts may also be too low. Based on observations at Kwajalein ( $8^{\circ} 40'N$ ), Barnes (1982) found that 'there is a thin persistent overcast of cirrus in the tropics most of the time.' It was almost always above the 14 km flight altitude and often could not be detected by ground observers except at sunrise and sunset. Even though it is thus 'sub-visible', its emissivity may not be negligible, judging from Figs. 4 and 5 of Paltridge and Platt (1981), since the infrared optical depth of a cloud is larger than the visible optical depth. However, Barnes (personal communication) estimates the ice-water content as 0.001 to 0.002  $g\ m^{-3}$ , and cloud thicknesses 0.2 to 1.0 km for these thin clouds. The IR emissivity, using Fig. 4 of Paltridge and Platt, would then be only 0.01 to 0.05. Sub-visible cirrus may thus have negligible effect on the radiation budget, compared with visible cirrus.

In order to obtain the average  $(T_s - T_c)$  given by the solid dot in Fig. 5 for July at  $5^{\circ}N$  cloud-top height,  $Z_c$ , needs to rise from 10.2 to 17.5 km (assuming  $\varepsilon = 0.5$ ) or to 12.0 km (assuming  $\varepsilon = 1.0$ ). Alternatively, it could be accomplished using London's  $Z_c = 10.2$  km and  $\varepsilon = 0.5$ , if the cirrus amount were increased from 23% to 60%. In summary, a climatology of cirrus cloud amount, height and emissivity would be very helpful to our understanding of the earth's radiation budget.

The other large discrepancy, at  $65^{\circ}S$  in July, may also be due to a wrong assumption of cloud-top height rather than of cloud amount. Even if the cloud amount were raised to 100%, the calculated outgoing IR would be only  $2\ W\ m^{-2}$  smaller than the 'partly cloudy' value plotted in Fig. 6. To reconcile calculation with observation at  $65^{\circ}S$  by changing cloud height instead of cloud amount it is necessary to assume that  $(T_s - T_c) = 25^{\circ}C$ , instead of  $7^{\circ}C$  as shown in Fig. 5. We do not know if this would be realistic, but admittedly, to take cloud heights observed at  $65^{\circ}N$  (predominantly land) and assume them to apply also at  $65^{\circ}S$  (predominantly ocean) is a dubious procedure. In addition, it is possible that our value of  $T_s$  is too high. The few surface observations available are ship reports from ice-free regions, where surface temperatures are unrepresentatively high.

These interpretations of the discrepancies are somewhat speculative because we ignore longitudinal asymmetry. In particular, if variations in cloud amount around a zone are correlated with variations in  $T_s$ , a bias will result that will be positive or negative depending on the sign of the correlation. In any case, the dip in zonal average IR is smaller than the average of dips at all longitudes, because the latitude of the ITCZ varies with longitude.

There is also the possibility that some of the error arises from inadequacy of observations due to poor sampling in time. Figure 1 of Bess *et al.* (1980) shows that outgoing IR radiation was sampled by Nimbus 6 on only about half the days in a typical month.

Finally, we note again that our calculations depend on biased and uncertain values of relative humidity, as discussed in section 3; some of the discrepancies are no doubt partly due to incorrect specification of relative humidity.

## 7. CONCLUSIONS

The tropical dip in outgoing IR radiation of  $20\text{--}40\ W\ m^{-2}$  is due not only to latitudi-

nal variation of cloud cover but also to latitudinal variation of tropospheric humidity. Radiative transfer model calculations suggest that about one third of the dip can be accounted for by humidity variation alone.

We have first shown what the IR dip would be if there were no clouds, and secondly shown the additional effect of clouds. The actual contribution of humidity to the observed dip will be less than these hypothetical clear-sky contributions because the water vapour greenhouse effect when it is cloudy will be affected only by humidity above the cloud. Since clouds cover about half the earth at any time, the actual contribution of humidity to the observed IR dip will be somewhat more than half the hypothetical contribution shown in Fig. 2.

However, a surprising finding of this study is that the dip is increased only slightly (to about  $12.3 \text{ W m}^{-2}$ , ignoring temporal and spatial variability) by the addition of clouds as specified by published cloud climatologies. Reconciliation of radiation calculations with satellite observations requires average cloud altitude, emissivity, or amount to be considerably higher than we have assumed, especially near the equator. In particular, we suspect that the cirrus heights given by London (1957) (and therefore our assumed cumulonimbus heights) for  $0-10^\circ$  are too low.

This study illustrates the need for better climatological data sets of both cloud and humidity, without which the sources of discrepancy between calculation and observation of outgoing IR cannot be identified. Global climatologies of cloud (including amounts by top-height and type) and relative humidity (including variability) are required.

An important part of a study of the climatology of RH would be to distinguish clear-sky RH from cloudy-sky RH, although Slingo (1980, Fig. 2) suggests that they may not be very different at an individual time and place. Our calculations in Figs. 2 and 6 used mean (clear and cloudy) relative humidities, but in order to separate more definitely the effects of clouds and RH, separate climatologies will be needed.

Cloud amount and relative humidity variations are probably correlated, at least for zonal monthly averages. Furthermore, we have shown that relative humidity variations have large effects on outgoing IR. Therefore, estimates of the effect of clouds on outgoing IR based on correlations of cloud amount variation with IR variation over latitude or season (Cess 1976, Cess *et al.* 1982) will tend to be over-estimates. This suggests that parametrizations of outgoing IR for use in simple climate models should explicitly include some measure of humidity as a predictor. Thompson and Warren (1982) do this, and they find that good estimates of clear-sky outgoing IR can be made with knowledge only of the surface air temperature and the  $0-12 \text{ km}$  height-mean relative humidity,  $\hat{R}H$ .

#### ACKNOWLEDGMENTS

This work was suggested by V. Ramanathan and sponsored by the Advanced Study Program and the Atmospheric Analysis and Prediction Division of the National Center for Atmospheric Research. The work was initiated while SGW was affiliated with the AAP of NCAR, and much of it was carried out while he was affiliated with the Cooperative Institute for Research in Environmental Sciences, University of Colorado. The work was supported at that time by a computing grant from NCAR to UC. Warren Wiscombe generously provided his ATRAD program for the radiative transfer calculations. Robert Cess, Garrett Campbell, Julius London and V. Ramanathan made helpful comments on the manuscript.

#### APPENDIX

##### *Temporal variability of relative humidity*

In order to estimate the day-to-day variability of  $\hat{R}H$  in section 5 we make use of estimates of interannual variability of monthly mean relative humidity, and the decay

time of the autocorrelation function of relative humidity. We use the monthly means of relative humidity obtained from radiosonde data in an unpublished study in 1978 by Warren. [We do not use the variability of individual 12-hourly soundings about the monthly mean, which he was studying, because this is largely due to *diurnal* variations, which, as pointed out in section 5, are here not relevant.]

TABLE 2. RADIOSONDE STATIONS USED AS DATA SOURCES FOR HUMIDITY VARIABILITY STATISTICS

Code in Figure 7	Station	Location	
A	Antofagasta, Chile	23°S	70°W
B	Balboa, Panama	9°N	79°W
C	Churchill, Manitoba, Canada	59°N	94°W
D	San Diego, California	33°N	117°W
E	Eniwetok Atoll	11°N	162°E
H	Hilo, Hawaii	20°N	155°W
I	Tripoli, Libya	33°N	13°E
J	San Juan, Puerto Rico	18°N	66°W
K	Keflavik, Iceland	64°N	23°W
L	Lake Charles, Louisiana	30°N	93°W
M	McMurdo, Antarctica	78°S	167°E
O	Okinawa, Japan	26°N	128°E
P	Puerto Montt, Chile	41°S	73°W
Q	Baker Lake, NWT, Canada	64°N	96°W
R	Resolute Bay, NWT, Canada	75°N	95°W
T	Topeka, Kansas	39°N	96°W
U	Huntington, West Virginia	38°N	82°W
Y	Yucca Flats, Nevada	37°N	116°W

Table 2 lists the radiosonde stations used. They were chosen to cover a wide variety of climatic regimes. Data were analysed for the 11-year period 1961–1971 at levels from surface to 500 mb. Values of  $\sigma(\overline{RH})$  are plotted in Fig. 7 as ordinate, with  $\overline{RH}$  as abscissa, where  $\overline{RH}$  is taken as the height-average for 0–6 km. We note that there is no correlation between  $\overline{RH}$  and  $\sigma(\overline{RH})$ , but that  $\sigma(\overline{RH})$  scatters between 0.03 and 0.10. We take  $\sigma(\overline{RH}) \approx 0.056$  as a representative mean value.

Simulations with the second-generation NCAR general circulation model indicate a characteristic autocorrelation decay time for variability of relative humidity which depends on latitude but has a global average of about two days for all levels in the troposphere (R. Chervin, personal communication). This means that the time,  $\tau$ , between independent samples is two days. The standard deviation of daily relative humidity,  $\sigma(\overline{RH})$ , is related to the standard deviation of monthly mean relative humidity,  $\sigma(\widehat{RH})$ , by  $\sigma(\overline{RH}) = \sigma(\widehat{RH})(30/\tau)^{1/2}$ , where  $\tau$  is two days. This gives us an estimate of  $\sigma(\overline{RH}) \approx 0.20$ , and we assume this value for the 0–6 km  $\overline{RH}$  to be valid also for the 0–12 km  $\widehat{RH}$ , i.e.  $\sigma(\widehat{RH}) \approx 0.20$ .

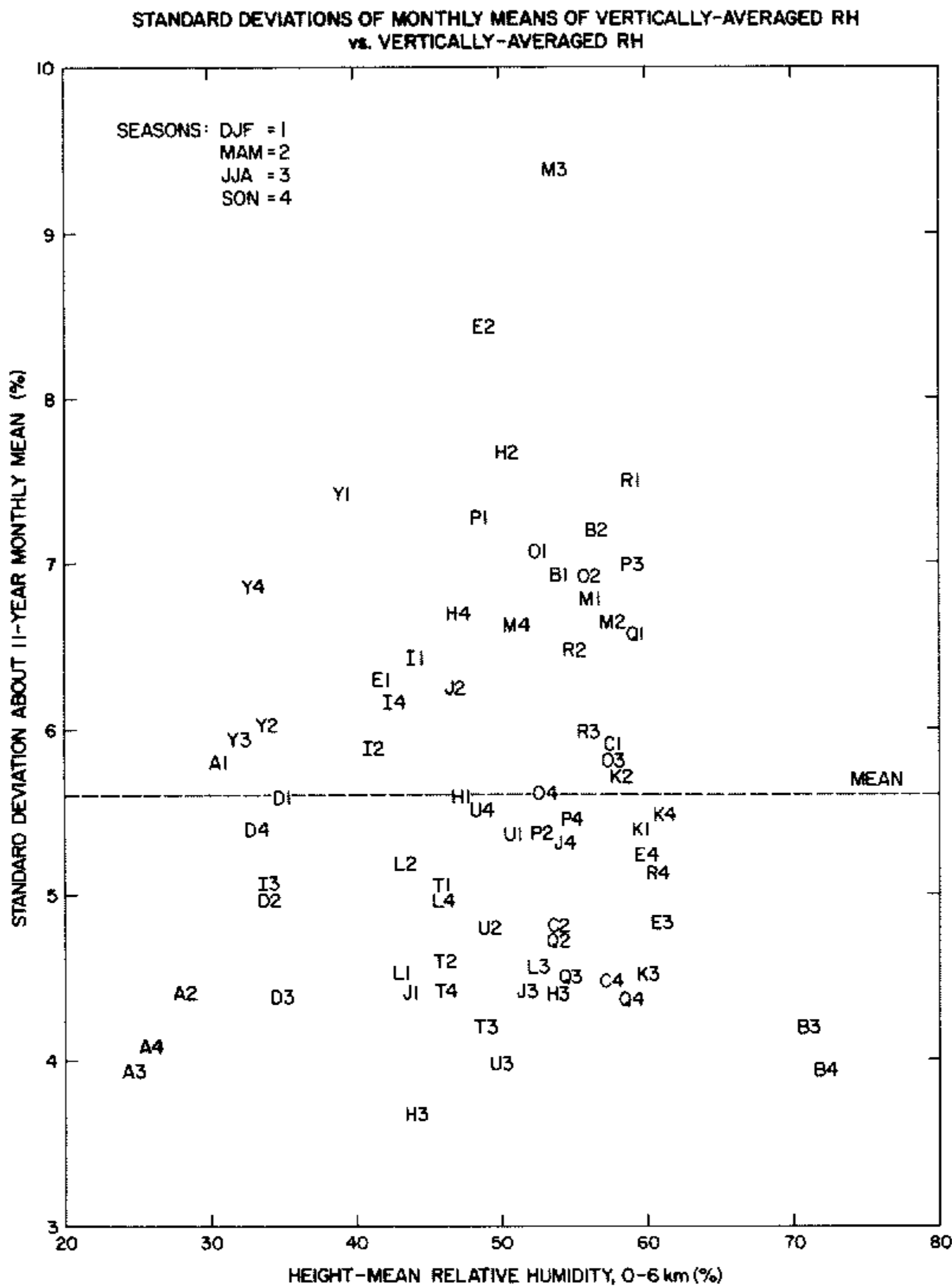


Figure 7. Standard deviation of monthly mean 0-6 km (height-mean) relative humidity about the long-term monthly mean, from radiosonde observations 1961-1971. The points are coded by number for season (1, 2, 3, 4 for DJF, MAM, JJA, SON, respectively) and by letter for station as given in Table 2.

#### REFERENCES

- |  |      |  |
|--|------|--|
| Barnes, A. A. Jr.                          | 1982 | The cirrus and subvisible cirrus background, <i>Second Symposium on the Composition of the Nonurban Troposphere</i> , American Meteorological Society, Boston, 170-175.      |
| Bess, T. D., Green, R. N. and Smith, G. L. | 1980 | <i>Deconvolution and analysis of wide-angle longwave radiation data from Nimbus 6 Earth Radiation Budget Experiment for the first year</i> , NASA Technical Paper 1746.      |
| Burch, D. E. and Gryvnak, D. A.            | 1979 | <i>Method of calculating H<sub>2</sub>O transmission between 333 and 633 cm<sup>-1</sup></i> , AFGL-TR-79-0054, Air Force Geophysics Laboratory, Hanscom AFB, Massachusetts. |
| Campbell, G. G. and Vonder Haar, T. H.     | 1980 | <i>An Analysis of Two Years of Nimbus 6 Earth Radiation Budget</i>   |

- Observations: July 1975 to June 1977, Atmos. Sci. Paper No. 320, Colorado State Univ., Fort Collins, CO.
- Cess, R. D. 1976 Climate change: An appraisal of atmospheric feedback mechanisms employing zonal climatology, *J. Atmos. Sci.*, **33**, 1831–1843.
- Cess, R. D., Briegleb, B. P. and Lian, M. S. 1982 Low-latitude cloudiness and climate feedback: comparative estimates from satellite data. *Ibid.*, **39**, 53–59.
- Cox, S. K. 1971 Cirrus clouds and the climate. *Ibid.*, **28**, 1513–1515.
- 1976 Observations of cloud infrared effective emissivity. *Ibid.*, **33**, 287–289.
- Crutcher, H. L. 1969 Temperature and humidity in the troposphere. *World Survey of Climatology*, Vol. 4, D. F. Rex (ed.), Elsevier, Amsterdam, 45–83.
- Danielsen, E. F. 1982 Statistics of cold cumulonimbus anvils based on enhanced infrared photographs. *Geophys. Res. Lett.*, **9**, 601–604.
- Ellingson, R. G. and Gille, J. C. 1978 An infrared radiative transfer model. Part 1: Model description and comparison of observations with calculations, *J. Atmos. Sci.*, **35**, 523–545.
- Griffith, K. T., Cox, S. K. and Knollenberg, R. G. 1980 Infrared radiative properties of tropical cirrus clouds inferred from aircraft measurements. *Ibid.*, **37**, 1077–1087.
- Griggs, M. 1968 Emissivities of natural surfaces in the 8- to 14-micron spectral region. *J. Geophys. Res.*, **73**, 7545–7551.
- Gruber, A. and Winston, J. S. 1978 Earth-atmosphere radiative heating based on NOAA scanning radiometer measurements. *Bull. Amer. Met. Soc.*, **59**, 1570–1573.
- Hunt, G. E. 1973 Radiative properties of terrestrial clouds at visible and infrared thermal window wavelengths. *Quart. J. R. Met. Soc.*, **99**, 346–369.
- Kneizys, F. X., Shettle, E. P., Gallery, W. O., Chetwynd, J. H. Jr., Abreu, L. W., Selby, J. E. A., Fenn, R. W. and McClatchey, R. A. 1980 *Atmospheric Transmittance/Radiance: Computer Code LOW-TRAN. 5*, AFGL-TR-80-0067, Air Force Geophysics Laboratory, Hanscom AFB, MA.
- Liou, K. N. 1974 On the radiative properties of cirrus in the window region and their influence on remote sensing of the atmosphere. *J. Atmos. Sci.*, **31**, 522–532.
- London, J. 1957 *A Study of the Atmospheric Heat Balance*, Report Contract AF 19(122)-165, College of Engineering, New York University, New York.
- McClatchey, R. A., Fenn, R. W., Selby, J. E. A., Volz, F. E. and Garing, J. S. 1972 *Optical Properties of the Atmosphere (Third Edition)*. AFCRL-72-0497, Air Force Geophysics Laboratory, Hanscom AFB, MA.
- Miranova, Z. F. 1973 Albedo of Earth's surface and clouds. *Radiation Characteristics of the Atmosphere and the Earth's Surface*, K. Ya. Kondrat'ev, (ed.), Amerind, New Delhi, 192–247.
- Murakami, T. 1975 Interannual cloudiness changes, *Mon. Weath. Rev.*, **103**, 996–1006.
- Oort, A. H. and Rasmusson, E. M. 1971 *Atmospheric Circulation Statistics*. NOAA Professional Paper No. 5, U.S. Dept. of Commerce, Rockville, MD.
- Paltridge, G. W. and Platt, C. M. R. 1981 Aircraft measurements of solar and infrared radiation and the microphysics of cirrus clouds. *Quart. J. R. Met. Soc.*, **107**, 367–380.
- Platt, C. M. R. and Stephens, G. L. 1980 The interpretation of remotely sensed high cloud emittances. *J. Atmos. Sci.*, **37**, 2314–2322.
- Ramanathan, V. 1977 Interactions between ice-albedo, lapse-rate and cloud-top feedbacks: an analysis of the nonlinear response of a GCM climate model, *J. Atmos. Sci.*, **34**, 1885–1897.
- Riehl, H. and Miller, A. H. 1978 Differences between morning and evening temperatures of cloud tops over tropical continents and oceans. *Quart. J. R. Met. Soc.*, **104**, 757–764.
- Roberts, R. E., Selby, J. E. A. and Biberman, L. M. 1976 Infrared continuum absorption by atmospheric water vapor in the 8–12  $\mu\text{m}$  window. *Appl. Optics*, **15**, 2085–2090.
- Sasamori, T., London, J. and Hoyt, D. V. 1972 Radiation budget of the Southern Hemisphere. *Meteorological Monographs*, **13**, 9–23.

- Selby, J. E. A., Shettle, E. P. and McClatchey, R. A. 1976 *Atmospheric Transmittance from 0.25 to 28.5  $\mu\text{m}$ : Supplement LOWTRAN 3B (1976) AFGL-TR-76-0258, Air Force Geophysics Laboratory, Hanscom AFB, MA 01731 USA.*
- Short, D. A. and Wallace, J. M. 1980 Satellite-inferred morning-to-evening cloudiness changes, *Mon. Weath. Rev.*, **108**, 1160–1169.
- Slingo, J. M. 1980 A cloud parametrization scheme derived from GATE data for use with a numerical model. *Quart. J. R. Met. Soc.*, **106**, 747–770.
- Stephens, G. L. 1980 Radiative properties of cirrus in the infrared region. *J. Atmos. Sci.*, **37**, 435–446.
- Stephens, G. L., Campbell, G. G. and Vonder Haar, T. H. 1981 Earth radiation budgets. *J. Geophys. Res.*, **86**, 9739–9760.
- Taljaard, J. J., van Loon, H., Crutcher, H. L. and Jenne, R. L. 1969 *Climate of the Upper Air: Southern Hemisphere. Vol. I. Temperatures, Dew Points, and Heights at Selected Pressure Levels.* NAVAIR 50-1C-55, U.S. Navy, Washington, D.C.
- Telegadas, K. and London, J. 1954 A physical model of the Northern Hemisphere troposphere for winter and summer. Scientific Report No. 1, AF 19(122)-165, College of Engineering, New York University, New York.
- Thompson, S. L. and Warren, S. G. 1982 Parameterization of outgoing infrared radiation derived from detailed radiative calculations. *J. Atmos. Sci.*, in press.
- van Loon, H. 1972 Cloudiness and precipitation in the Southern Hemisphere. *Meteorological Monographs*, **13**, 101–111.
- Warren, S. G., Hahn, C. and London, J. 1981 Ground-based observations of cloudiness for cross-validation of satellite observations. *Clouds in Climate*, NASA-GISS, New York, 174–179.
- Warren, S. G. and Schneider, S. H. 1979 Seasonal simulation as a test for uncertainties in the parameterizations of a Budyko–Sellers zonal climate model. *J. Atmos. Sci.*, **36**, 1377–1391.
- Wiscombe, W. J. 1975 Solar radiation calculations for Arctic summer stratus conditions. *Climate of the Arctic*, G. Weller and S. A. Bowling (eds.), Geophysical Institute, Univ. of Alaska, Fairbanks, AK, 245–254.
- 1976 Extension of the doubling method to inhomogeneous sources. *J. Quant. Spectr. and Rad. Trans.*, **16**, 447–489.
- Wiscombe, W. J. and Evans, J. W. 1977 Exponential-sum fitting of radiative transmission functions. *J. Comp. Phys.*, **24**, 416–444.